ADVANCED HEALTHCARE MATERIALS
www.advhealthmat.de

Effect of Particle Size and Surface Chemistry of Photon-Upconversion Nanoparticles on Analog and Digital Immunoassays for Cardiac Troponin

Julian C. Brandmeier, Kirsti Raiko, Zdeněk Farka, Riikka Peltomaa, Matthias J. Mickert, Antonín Hlaváček, Petr Skládal, Tero Soukka,* and Hans H. Gorris**

Sensitive immunoassays are required for troponin, a low-abundance cardiac biomarker in blood. In contrast to conventional (analog) assays that measure the integrated signal of thousands of molecules, digital assays are based on counting individual biomarker molecules. Photon-upconversion nanoparticles (UCNP) are an excellent nanomaterial for labeling and detecting single biomarker molecules because their unique anti-Stokes emission avoids optical interference, and single nanoparticles can be reliably distinguished from the background signal. Here, the effect of the surface architecture and size of UCNP labels on the performance of upconversion-linked immunosorbent assays (ULISA) is critically assessed. The size, brightness, and surface architecture of UCNP labels are more important for measuring low troponin concentrations in human plasma than changing from an analog to a digital detection mode. Both detection modes result approximately in the same assay sensitivity, reaching a limit of detection (LOD) of 10 pg mL^{-1} in plasma, which is in the range of troponin concentrations found in the blood of healthy individuals.

1. Introduction

Heart diseases such as acute myocardial infarction (AMI) are the leading cause of death worldwide.[1] Since there is only a limited time available from the onset of the symptoms to lifesaving treatment, fast and reliable diagnostic tests are essential. In healthy individuals, cardiac troponin (cTn) is located exclusively in myocardial tissue. Therefore, several clinical tests have been employed to measure elevated levels of cTn—the recommended biomarker for AMI—in blood for the early diagnosis of AMI.[2] cTn is a heterotrimeric complex consisting of cTnI, cTnT, and TnC.[3,4] The subunits cTnI and cTnT exist as unique, recognizable isoforms only in the heart muscle (myocardium) and are released into the blood during AMI.[5,6] Highly sensitive, precise, and specific troponin tests are required to discriminate between low cTnI levels in blood and background noise.[7] Commercial chemiluminescence, electrochemical, or fluorescence assays in clinical use[8] reach limits of detection (LOD) in the range of 0.08–2.7 pg mL^{-1}.[9] According to the European Society of Cardiology and the American College of Cardiology, increased cTnI or cTnT levels in blood are defined as the value above the 99th percentile concentration of a healthy reference population, which varies typically between 8.67 and 60.4 pg mL^{-1}.[10,11]

Nevertheless, cTnI is a challenging analyte for immunochemical detection, and quantitative measurements can be influenced by several factors, such as the availability of epitopes for antibody binding. Due to the proteolytic susceptibility of the N- and C-terminal parts of cTnI,[12] antibodies for cTnI assays are often selected to recognize epitopes in the stable central part.[13,14] Furthermore, since cTnI in the blood is mainly present as a binary cTnI–TnC complex,[8] the antibodies should recognize both the free and complexed forms of cTnI. Moreover, phosphorylation or blocking of the epitopes by autoantibodies or heterophile antibodies may hinder the antibody recognition.[15] As it is unlikely that a single antibody pair is not affected by some kind of cTnI modifications or interferences,[16] many cTnI assays use a combination of two capture or two detection antibodies.[9] Furthermore, troponin assays often suffer not only from a low working range but also from rather poor precision at concentrations

J. C. Brandmeier, Z. Farka, R. Peltomaa, M. J. Mickert, H. H. Gorris
Institute of Analytical Chemistry, Chemo- and Biosensors
University of Regensburg
Regensburg 93053, Germany
E-mail: farka@mail.muni.cz; hans-heiner.gorris@ur.de
K. Raiko, R. Peltomaa, T. Soukka
Department of Life Technologies/Biotechnology
University of Turku
Kiinamyllynkatu 10, Turku 20520, Finland
E-mail: tejoso@utu.fi
Z. Farka, P. Skládal
Department of Biochemistry, Faculty of Science
Masaryk University
Kamenice 5, Brno 625 00, Czech Republic
A. Hlaváček
Institute of Analytical Chemistry of the Czech Academy of Sciences
v. v. i., Brno 602 00, Czech Republic

The ORCID identification number(s) for the author(s) of this article can be found under https://doi.org/10.1002/adhm.202100506

DOI: 10.1002/adhm.202100506

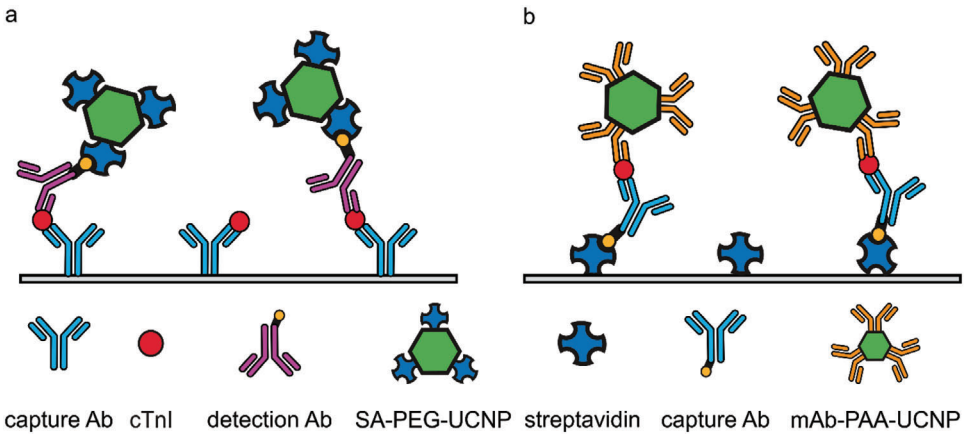

Figure 1. ULISA configurations for the detection of cardiac troponin (cTnI). a) SA-PEG-UCNP label: A microtiter well is coated with monoclonal mouse anti-cTnI antibodies to capture cTnI. The biotinylated anti-cTnI antibody binds to cTnI and forms a sandwich immunocomplex, which is detected using SA-PEG-UCNP labels. b) mAb-PAA-UCNP label: A microtiter well is coated with streptavidin to immobilize biotinylated anti-cTnI antibodies, which capture cTnI. Finally, mAb-UCNP conjugates bind to cTnI and form a sandwich immunocomplex.

below the 99th percentile.[17] The choice of signal-generating labels is of a paramount importance to improve the assay reliability and performance.

Photon-upconversion nanoparticles (UCNP) represent lanthanide-doped luminescent labels emitting shorter-wavelength light under near-infrared excitation (anti-Stokes emission), which strongly reduces background interference because of autofluorescence and light scattering.[18,19] Due to these remarkable optical properties, UCNPs are excellent labels for upconversion-linked immunosorbent assays (ULISA).[20–22] The hydrophobic layer of oleic acid on pristine UCNPs needs to be replaced by a hydrophilic coating to render the UCNPs dispersible in aqueous media and allow further bioconjugation. Alkyne-poly(ethylene glycol) (PEG) conjugated to neridronate, a bisphosphonate, has been shown to strongly coordinate to surface lanthanide ions of UCNPs. The alkyne group reacts with azide-modified streptavidin via click-chemistry.[23,24] Alternatively, surface coating with hydrophilic poly(acrylic acid) (PAA) yields water-dispersible nanoparticles with excellent colloidal stability and high density of surface carboxyl groups for bioconjugation via EDC/NHS activation.[25]

Furthermore, the absence of optical background interferences enables the detection and counting of individual UCNP labels using wide-field optical microscopy.[19,26] This has led to the development of single-molecule (digital) immunoassays,[27] as opposed to analog immunoassays where the integrated signal generated by thousands of labels is measured. It is essential that the UCNP labels have the right size and are bright enough to be reliably detectable (and countable) at the single-nanoparticle level. If this condition is met, the digital assay is essentially independent of varying particle brightness, particle aggregation, and the instrumental background. With high-affinity detection antibodies, the LOD is limited by (1) the standard deviation of the nonspecifically bound labels in the control sample without analyte, and (2) counting statistics, as the precision of the measurement depends on the number of counted events (Poisson noise).

We previously developed a digital ULISA with PEG-neridronate-based UCNP labels for the detection of prostate-specific antigen (PSA).[19,26] The digital readout yielded an LOD of 0.023 pg mL^{-1}, which was 20-fold more sensitive than the analog readout. In another study, we applied PAA-coated UCNPs to the detection of cTnI in the analog mode, which resulted in an LOD of 0.48 pg mL^{-1}.[28,29] Here, we employ both surface modification strategies for UCNPs and critically assess the effect of the UCNP label size on the performance of the analog and digital immunoassay for cTnI. The schemes of the sandwich ULISAs using either type of label are shown in **Figure 1**.

2. Experimental Section

2.1. Chemicals and Reagents

A complete list of chemicals and the preparation of alkyne-PEG-neridronate (Alkyne-PEG-Ner) and the streptavidin-azide are provided in the Supporting Information. The cTn I-T-C complex, and monoclonal anti-cTnI-antibody (mAb) clones 19C7cc, MF4cc, 560cc, and 625cc were purchased from Hytest (Turku, Finland). The mAbs 560cc and 625cc were biotinylated as described in the Supporting Information and mAb 19C7 as previously published.[30] The recombinant anti-cTnI F_{ab} fragment 9707 was cloned from a hybridoma cell line of Medix Biochemica (Espoo, Finland) and produced and site-specifically biotinylated as described previously.[31] Blood for the plasma pool from five anonymized healthy volunteers was collected in lithium-heparin vacuum tubes (BD Vacutainer 10 mL, Plymouth, UK). Volunteers provided written informed consent regarding the use of collected plasma samples according to the principles expressed in the Declaration of Helsinki. Plasma was stored at −20 °C, and the aliquots were freshly thawed and centrifuged for 5 min at 1000 *g* before each experiment. The STAT troponin I test (Abbot, Chicago, IL, USA) was used to determine the intrinsic cTnI concentration in plasma.

The buffers were prepared using double-distilled water and filtered through a 0.22-µm membrane (Magna Nylon, GVS, USA). The buffers for the dilution of reagents included phosphate buffer (PB; 50×10^{-3} M NaH_2PO_4/Na_2HPO_4, pH 7.4), phosphate-buffered saline (PBS; PB with 150×10^{-3} M NaCl), Tris-buffered saline (TBS; 50×10^{-3} M Tris, 150×10^{-3} M

NaCl, pH 7.5). Coating buffer consisted of 50×10^{-3} M $NaHCO_3/Na_2CO_3$, 0.05% NaN_3, pH 9.6. Two types of washing buffers were employed: Kaivogen-washing buffer and Tris-washing buffer (50×10^{-3} M Tris, 5×10^{-3} M $CaCl_2$, 0.05% Tween 20, pH 7.5). Several assay buffer combinations were investigated: (1) SuperBlock buffer (10% SuperBlock in TBS, 1×10^{-3} M KF, 0.05% Tween 20, 0.05% PEG, and 0.05% NaN_3, pH 7.5), (2) SuperBlock buffer with 5×10^{-3} M $CaCl_2$ (SuperBlock-Ca), (3) Kaivogen assay buffer, (4) modified Kaivogen assay buffer (assay buffer including 0.05% PAA (M_W 1200 Da), 1×10^{-3} M KF, 0.2% milk powder, 0.08% native mouse IgG, 0.005% denatured mouse IgG, pH 8.0), (5) BSA/BGG buffer (37.5×10^{-3} M Tris, 513×10^{-3} M NaCl, 5% D-trehalose, 2.5% BSA, 0.06% BGG, 0.04% NaN_3, pH 8.6), and (6) BSA/BGG/IgG buffer (37.5×10^{-3} M Tris, 500×10^{-3} M NaCl, 5% D-trehalose, 2.5% BSA, 0.06% BGG, 0.08% native mouse IgG, 0.005% denatured mouse IgG, 0.2% casein, 37.5 U mL^{-1} heparin, 0.0375% NaN_3, pH 7.75). Calibrator dilutions were prepared in 7.5% BSA/TSA (50×10^{-3} M Tris, pH 7.75, 150×10^{-3} M NaCl and 0.05% NaN_3, with 7.5% BSA).

2.2. Preparation of and Characterization of UCNP Labels

2.2.1. SA-PEG-UCNP Conjugates

For the preparation of SA-PEG-UCNP labels, UCNPs ($NaYF_4$:Yb,Er, 63 nm in diameter) were synthesized as described in the Supporting Information. The UCNPs (10 mg, 311 µL) dispersed in cyclohexane were mixed with an equal volume of 200×10^{-3} M HCl and incubated for 30 min at 38 °C under shaking and an additional 15 min of sonication to remove the oleic acid from the UCNP surface and mediate a phase transfer from cyclohexane to water. The lower HCl phase was added to an excess of acetone and centrifuged (1000 *g*, 20 min) to precipitate the UCNPs. The UCNP pellet was redispersed in 500 µL of water, sonicated for 5 min, and 2 mg of the Alkyne-PEG-Ner linker dissolved in 500 µL of water were added and incubated overnight at 38 °C under shaking. The Alkyne-PEG-Ner-UCNP conjugates were dialyzed for 72 h in a Float-A-Lyzer G2 dialysis device (100 kDa M_W cut-off; Fisher Scientific) at 4 °C against 4 L of 1×10^{-3} M KF in water, which was exchanged nine times.

For the functionalization with streptavidin, 100 µL of Tris-HCl (375×10^{-3} M, pH 7.5) and an aqueous solution of sodium ascorbate (20 µL, 100×10^{-3} M) were added to 10 mg of Alkyne-PEG-Ner-UCNPs in 1.4 mL of water. After purging the mixture for 45 min with argon, 100 µL of streptavidin-azide (1 mg mL^{-1} in water) were added, and the mixture was purged for another 10 min. Adding 10 µL of an aqueous solution of 25×10^{-3} M $CuSO_4$ initiated the click reaction. The suspension was purged for 40 min with argon and then dialyzed in a Float-A-Lyzer G2 dialysis device (100 kDa M_W cut-off) against 4 L of dialysis buffer (50×10^{-3} M Tris, 0.05% NaN_3, 1×10^{-3} M KF, pH 7.5 at 4 °C for 72 h), which was exchanged nine times.[32]

2.2.2. mAb-PAA-UCNP Conjugates

For the preparation of mAb-PAA-UCNP labels, oleic acid-capped UCNPs ($NaYF_4$:Yb,Er; 40, 48, 56, 64, and 80 nm in diameter) were obtained from Kaivogen. The oleic acid was removed and replaced with PAA in a two-step ligand exchange with $NOBF_4$, as described previously.[33] The UCNPs (25 mg) dispersed in cyclohexane were mixed with an equal volume of dimethylformamide (DMF). The suspension was sonicated for 1 min, added to 25 mg of $NOBF_4$ and vortexed vigorously. During the following 60 min under shaking (1200 rpm), oleic acid on the nanoparticle surface was replaced by BF_4^-, which mediated a phase transfer from cyclohexane to DMF. The UCNP dispersion was split into two aliquots and the particles were precipitated by adding a fourfold volume excess of chloroform to the dispersion in DMF. The UCNPs were washed four times by alternating precipitation with chloroform and centrifugation (11 000 *g*, 5 min) followed by redispersion in 200 µL of DMF. The UCNP pellet was resuspended in 150 µL DMF, centrifuged (2500 *g*, 3 min) to remove possible larger aggregates, and the supernatant was transferred to a fresh tube. The yield of UCNPs coated with BF_4^- was determined by comparing the luminescence of the solution to that of 10 mg mL^{-1} UCNP standard, both diluted 200 times in 10×10^{-3} M $B_4Na_2O_7$, pH 8 with 0.1% Tween-20).

The DMF dispersion of BF_4^--coated UCNPs was mixed with a 10% solution of poly(acrylic acid) (PAA, M_W 2000) in water (adjusted to pH 9 by NaOH) such that a twofold mass excess of PAA compared to UCNPs was obtained. The mixture was further diluted with DMF to yield a PAA concentration of 3.3% and incubated for 24 h at 60 °C under shaking (1400 rpm). The PAA-coated UCNPs were washed three times by centrifugation (20 000 *g*, 15 min) and resuspended twice in 1 mL of water and finally in 1 mL of sodium borate buffer (50×10^{-3} M H_3BO_3 with NaOH, pH 8.0). This suspension was centrifuged once more at lower speed (2500 *g*, 3 min) to sediment possible larger aggregates. The supernatant was carefully collected and stored at room temperature (RT) until further use.

The conjugation of mAb 625cc and mAb 560cc was adapted from a previously published protocol[28] and all steps were performed at RT. A dispersion of 250 µL of PAA-coated UCNPs (2 mg) in 20×10^{-3} M aqueous MES buffer (pH 6.1) was activated using 20×10^{-3} M EDC and 30×10^{-3} M sulfo-NHS for 45 min under shaking. The UCNPs were washed by two centrifugation steps (20 000 *g*, 7 min), the initial one followed by resuspension in 335 µL and the second in 210 µL of 20×10^{-3} M MES buffer. 40 µL of mAbs solution in 0.9% NaCl was added to yield a final antibody concentration of 0.33 mg mL^{-1} in a total volume of 250 µL. After 2.5 h under rotation, an aqueous solution of 2 M 2-amino-*N*,*N*-dimethylacetamide (ADMA) in water (pH 11) was added to yield a final ADMA concentration of 50×10^{-3} M. The mixture was rotated for 30 min to terminate the conjugation reaction and block the nanoparticle surface. After washing twice by centrifugation (20 000 *g*, 10 min) and resuspension in 500 µL of Tris-buffer (10×10^{-3} M Tris, 0.1% Tween 20, pH 8), the antibody-conjugated UCNPs (mAb-PAA-UCNPs) were resuspended in 5×10^{-3} M Tris, pH 8.5, 0.05% Tween 85, 0.5% BSA, 0.05% NaN_3, pH 8.5, and stored at 4 °C.

2.2.3. Characterization of UCNP Labels

The UCNPs and their conjugates were characterized using transmission electron microscopy (TEM), dynamic light scattering

(DLS), and upconversion emission spectroscopy as described in Figures S1–S3 in the Supporting Information.

2.3. ULISA

2.3.1. SA-PEG-UCNP Labels

A high-binding 96-well microtiter plate (μClear with 190-μm-thick bottom foil for microscope detection, Greiner, Austria) was coated with 60 µL of two monoclonal anti-cTnI antibodies (19C7cc and MF4cc, each 50 ng/well) in coating buffer overnight at 4 °C. The following steps were carried out at RT. The plate was washed twice with 250 µL of Tris-washing buffer and blocked for 1 h with 175 µL of SuperBlock buffer. After two washing steps, the cTn I-T-C complex was serially diluted in 60 µL of either BSA/BGG buffer alone, or 20% human plasma in BSA/BGG buffer and incubated for 1 h. The microtiter plate was washed twice and incubated for 1 h with 60 µL of a mixture containing biotinylated anti-cTnI antibodies (560cc and 625cc; each 0.5 µg mL^{-1}) in SuperBlock-Ca buffer. After two washing steps, the plate was incubated with 60 µL of SA-PEG-UCNPs (6.5 µg mL^{-1}) for 1 h in SuperBlock-Ca buffer. After two washing steps, the plate was left to dry on air.

2.3.2. mAb-PAA-UCNP Labels

All steps were carried out at RT. The mAb-PAA-UCNP labels were diluted 30 min before starting the assay in modified Kaivogen assay buffer to a final concentration of either 4 µg mL^{-1} of mAb625-PAA-UCNP alone, or 2 µg mL^{-1} of each label in a mixture of mAb625-PAA-UCNP and mAb560cc-PAA-UCNP.

A high-binding 96-well microtiter plate (μClear with 190-µm-thick bottom foil for microscope detection, Greiner) was coated with streptavidin as described earlier.[34] The plates were first washed with Kaivogen washing buffer. Then, 50 µL of biotinylated mAb 19C7cc (150 ng/well) and F_{ab} 9707 (50 ng/well) in Kaivogen assay buffer were added and incubated for 30 min under shaking. After one washing step, the cTn I-T-C complex was serially diluted in 50 μL/well in 7.5% BSA/TSA or human plasma, respectively, followed by further dilution to 20% in BSA/BGG/IgG buffer, and incubated for 30 min. After one washing step, the mAb-PAA-UCNP labels prepared prior to the assay were sonicated 3× for 0.5 s with 100% amplitude using a VialTweeter (Hielscher Ultrasonics, Teltow, Germany) and added to the microtiter plate (50 μL/well). After 15 min, the microtiter plate was washed four times and left to dry on air.

2.4. Signal Acquisition and Statistical Analysis

2.4.1. Analog Readout

A modified upconversion microtiter plate reader (Chameleon, Hidex, Turku, Finland) equipped with a 980-nm laser excitation source[35] was used for measuring the integrated emission of Er-doped UCNPs at 540 nm. (1) In the case of SA-PEG-UCNP labels, 64 points were scanned in each well with a distance of 100 µm and a signal integration time 1 s. Afterwards, the 16 highest and 16 lowest values were discarded, and the mean value was calculated, providing the truncated average of the intensity in a single well. (2) In the case of mAb-PAA-UCNP labels, the bottom surface of the microtiter plate wells was scanned using a 3 × 3 raster with 1.5 mm step size and an exposure time of 2 s and the average intensity per well was calculated. The plotted averages and standard deviations (mean ± SD) were determined from three independent wells. The data was fitted by a four-parameter logistic function using the software Origin 2020 (OriginLab, USA). The LODs were obtained by adding three times the standard deviation of the background to the baseline values of the regression curve.[26]

2.4.2. Digital Readout

An inverted wide-field epifluorescence microscope (Eclipse Ti, Nikon, Japan) was connected to a continuous-wave 980-nm laser diode (4 W, Wavespectrum, China) via a multimode optical fiber (105 µm fiber core, 0.22 NA, Wavespectrum) and a motorized TIRF/Epifluorescence illuminator unit (Eclipse Ti-E, Nikon, Japan). The filter cube for the detection of Er^{3+}-doped UCNPs consisted of a long-pass excitation filter ($\lambda_{cut\text{-}on}$ = 830 nm, Schott, Germany), a dichroic mirror ($\lambda_{cut\text{-}on}$ = 875 nm, AHF Analysentechnik, Germany), and a band-pass filter (λ = 535 ± 70 nm, $OD_{980} \approx 6$, Chroma, USA). The images were acquired on an sCMOS camera (5.5 megapixel, Neo, Andor Technology, UK) and a 100× objective (1.49 NA, CFI HP Apochromat TIRF, Nikon), which resulted in a power density of 640 W cm^{-2}.

The dry microtiter plate wells were filled with 80 µL of glycerol for heat dissipation of the NIR laser beam. The software NIS Elements 4.5 (Nikon) was used for the acquisition of 9 wide-field images per well with an imaging area of 166 × 144 μm^2 and exposure times between 10 and 30 s (depending on the size—and thus brightness—of the UCNPs)[19] and for the counting of individual UCNPs. The total number of UCNPs per well (n = 3) was analyzed using a four-parameter logistic function in Origin 2020. The LODs were obtained by adding three times the standard deviation of the background to the baseline values of the regression curve.[26]

3. Results and Discussion

3.1. Optimization of Antibody Combination and ULISA Configuration

cTnI is a very fragile analyte prone to proteolytic degradation, phosphorylation, or complexing with other proteins and autoantibodies.[16,36–38] As these factors are not relevant when cTnI is present in well-defined buffers, it is necessary to assess the detectability of cTnI in its physiological environment, where many different enzymes, troponins, and other proteins are present in varying concentrations. Therefore, we prepared a plasma pool from five healthy volunteers and determined the intrinsic cTnI concentration using a commercial test (28.8 pg mL^{-1}) to distinguish it from spiked troponin concentrations.

The immunoassay performance further depends on the careful selection of antibodies and the assay configuration. We first

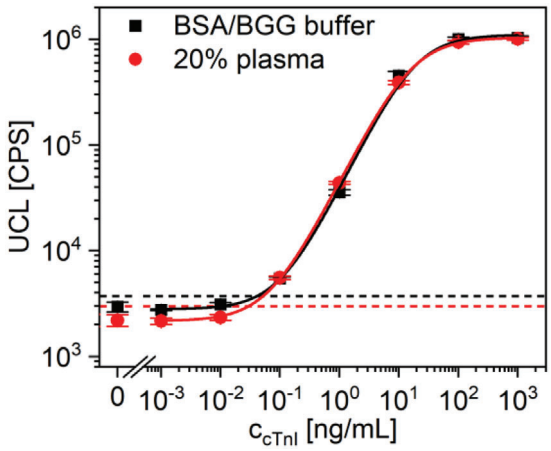

Figure 2. Calibration curves of the analog ULISA using biotinylated mAb 560cc and SA-PEG-UCNP labels. cTnI was serially diluted in either BSA/BGG buffer (LOD: 41 pg mL^{-1}; bg: 3000 CPS), or first in 20% plasma and then in BSA/BGG buffer (LOD: 30 pg mL^{-1}; bg: 2200 CPS). The error bars show the standard deviation of three replicate measurements (mean ± SD, $n = 3$). The hatched lines indicate the LODs.

coated the capture antibodies mAb 19C7cc and MF4cc directly on the microtiter plate surface (Figure 1a). cTnI was then detected using biotinylated detection antibodies and SA-PEG-UCNP labels. When comparing the biotinylated detection antibodies mAb 560cc, mAb 625cc, and a combination of both, mAb 625cc alone was sufficient to achieve the highest sensitivity (Figure S4a, Supporting Information). **Figure 2** shows the calibration curves of cTnI either prepared in BSA/BGG buffer or in 20% plasma and then diluted in BSA/BGG buffer. The LODs of the assay were 41 pg mL^{-1} in BSA/BGG buffer (corresponding to 120 pg mL^{-1} in undiluted sample) and 30 pg mL^{-1} in 20% human plasma (corresponding to 80 pg mL^{-1} in undiluted sample). The only difference between the calibration curves is the slightly lower background (bg) signal as a result of blocking effects of serum proteins, which has a positive effect on the LOD measured in plasma samples. The assay, however, shows no cross-reactivity towards other proteins in plasma, which would have increased the background signal.

In the second assay configuration (Figure 1b), we used streptavidin for coating the microtiter plate surface. Independent of a partial denaturation during the adsorption-based surface attachment, at least one of the four high-affinity binding sites of streptavidin is usually available for binding of biotin. At the same time, the streptavidin layer affords the right orientation of the biotinylated antibody. This is especially important for binding of small biotinylated F_{ab} fragments, which may lose their activity through denaturation after direct adsorption-based surface attachment. In this configuration, we employed a combination of biotinylated F_{ab} 9707 and biotinylated mAb 19C7cc. The smaller size of the F_{ab} fragment enhanced the epitope availability for the detection antibody.[12] On the detection side, two types of mAb-PAA-UCNP labels were compared, one carrying mAb 560cc on the nanoparticle surface and the other mAb 625cc. A combination of both antibody conjugates was also investigated. The LOD was rather independent of the label type in the buffer (Figure S4, Supporting Information), but mAb 625cc-PAA-UCNP resulted in a higher sensitivity in plasma (data not shown) and thus was used for further experiments.

3.2. Effect of UCNP Label Size

The size of the UCNP-based detection label is another important parameter influencing the immunoassay performance. On the one hand, the size should be small to (1) obtain stable nanoparticle dispersions, (2) reduce nonspecific binding, and (3) minimize their influence on the antibody–antigen interaction. On the other hand, a larger size of UCNPs strongly increases their brightness such that they can be more easily detected. The brightness is particularly important for the detection of the labels at the single-nanoparticle level. Therefore, we conjugated UCNPs of 40, 48, 56, 64, and 80 nm in diameter to mAb 625cc and used them as labels for the detection of cTnI in buffer (**Figure 3**a) and in human plasma (Figure 3b).

While the background signal of mAb-PAA-UCNP labels in BSA/BGG/IgG buffer was in general lower (<2000 CPS) than for the SA-PEG-UCNP labels in buffer and only increased slightly with the label size (see **Table 1** for a detailed comparison), the use of plasma resulted in a ten times higher background signal when the label size increased from 40 to 80 nm. Also, a comparison among the same label sizes showed that the background was 2–20 times higher in plasma than in the buffer. Therefore, the higher background signal of larger UCNP labels cannot be simply explained by a higher brightness of larger UCNPs, but is rather a consequence of plasma components leading to a higher level of nonspecific binding of the larger particles to the microtiter plate. The higher LOD of the ULISA with larger UCNP labels in plasma can be attributed to the higher background signal. The origin of the increased tendency to nonspecific binding of the larger UCNPs may be related to the larger contact area (affected also by the shape of the nanoparticles) with the surface, which may lead a larger number of simultaneous weak interactions.

3.3. Performance of Digital Assays

In our previous work on PSA,[26] we observed that counting single immunocomplexes (digital mode, LOD: 0.02 pg mL^{-1}) resulted in a 20-fold higher sensitivity than the analog mode (LOD: 0.4 pg mL^{-1}) using SA-PEG-UCNP detection labels in the same configuration as shown in Figure 1a. We explained the higher sensitivity of the digital mode by the reduced influence of label aggregation in the digital mode, where each aggregate—independent of its size—is counted only as a single binding event. In the analog mode, by contrast, an aggregate bound nonspecifically to the microtiter plate surface can strongly increase the background signal depending on the number of UCNPs in the aggregate.

In our current work, the same microtiter plates prepared for the analog detection of troponin were used for counting individual cTnI immunocomplexes under the upconversion microscope to determine the concentration in the digital mode. **Figure 4** shows microscope images of single immune complexes labeled with mAb-PAA-UCNPs (56 nm; images of other mAb-PAA-UCNP sizes and SA-PEG-UCNPs are shown in Figures S5 and

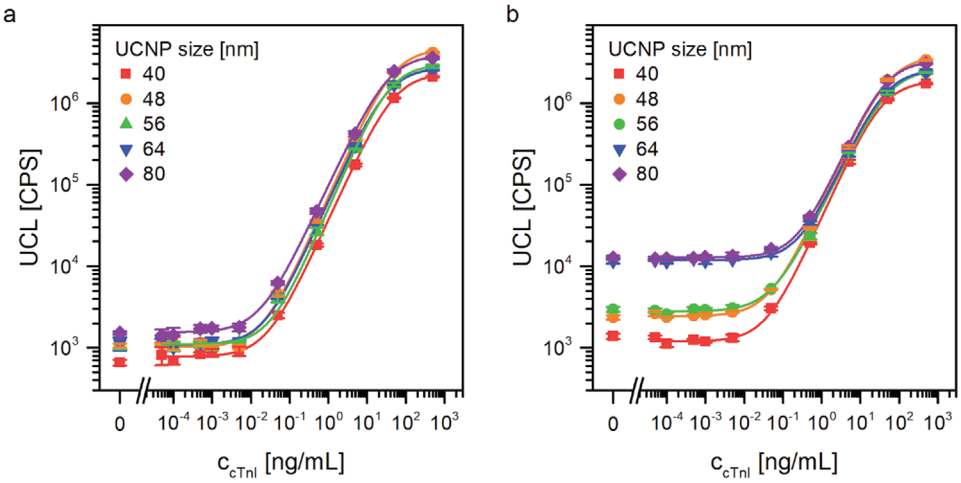

Figure 3. Analog ULISA for the detection of cTnI using different sizes of UCNP-PAA conjugated to mAb 625cc in a) buffer and b) 20% plasma. The error bars show standard deviations of replicate measurements in three wells (mean ± SD, $n = 3$).

Table 1. Summary of the analog and digital detection of cTnI in buffer and in human plasma using mAb-PAA-UCNP labels.

Detection of cTnI	in buffer				in plasma			
	analog		digital		analog		digital	
UCNP size[a] [nm]	background signal (CPS)	LOD [pg mL^{-1}]	number of UCNPs[b]	LOD [pg mL^{-1}]	background signal (CPS)	LOD [pg mL^{-1}]	number of UCNPs[b]	LOD [pg mL^{-1}]
40	658	6.0	n.d.[c]	n.d.[c]	1387	11.9	n.d.[c]	n.d.[c]
48	1055	3.8	33	3.3	2622	8.6	105	9.8
56	1038	8.3	21	7.0	2958	11.8	74	65.2
64	1129	13.3	15	17.4	11211	57.2	209	17.2
80	1517	2.9	15	4.7	12716	44.9	153	160.0

[a] Average UCNP diameter determined by TEM (Figure S1, Supporting Information); [b] Number of luminescent spots in the background images (0.2 mm^2). Average of 3 wells calculated from the sum of 9 images per well; [c] Not determinable because smaller UCNPs are not bright enough for single-nanoparticle detection.

S6 in the Supporting Information). A minimal size of 48 nm was required for a reliable detection at the single-nanoparticle level. In both buffer and plasma, the distribution of the label brightness was relatively uniform among different types and sizes of labels (Table S1, Supporting Information), indicating that the number of aggregates present in the label samples was relatively small.

The calibration curves of the digital assays are summarized in **Figure 5**. In contrast to the analog readout (Figure 3), the number of nonspecifically bound labels was relatively independent of the label size in BSA/BGG/IgG buffer and in plasma (Figure 5, Table 1). While most of the increased background is a result of more nonspecific binding events in plasma, it should be noted that in the case of small nanoparticles, also the average brightness per diffraction-limited spot increased, which indicates that the plasma has an indirect effect on the label aggregation (Table S1, Supporting Information). As the background mainly determines the assay sensitivity, the sensitivity of the digital detection in buffer was relatively similar among the different label sizes. By contrast, the assay sensitivity decreased in plasma when using larger labels, with exception of the 64-nm conjugates.

We also compared the assay performance in the digital mode using SA-PEG-UCNP labels (Figure S7, Supporting Information), but these labels did not improve the LOD compared to the analog readout (Figure 2), either. Therefore, independent of the assay configuration and the type and size of the label, the analog and digital readout resulted in similar LODs. The number of nonspecifically bound mAb-PAA-UCNP labels in the background image of the blank sample (Figure 5a) was about ten times lower than the number of nonspecifically bound SA-PEG-UCNP labels (Figure S7, Supporting Information), which was consistent with our earlier PSA experiments using SA-PEG-UCNP labels.[26] The lower number of counting events (n) increased the Poisson noise ($\sqrt{n}/n$) and affected the accuracy of the digital readout. For example, in the case of 64-nm UCNPs and 80-nm UCNP, the nonspecific binding was so low that only 15 diffraction-limited spots were detectable in the imaging area. A count of 15, however, results in a relatively high Poisson noise of 26%. In Figure 5a, the lowest baselines show the highest fluctuations, due to the Poisson noise.

An explanation why the digital readout improved the LOD of the PSA assay but not the LOD of the troponin assay may be that

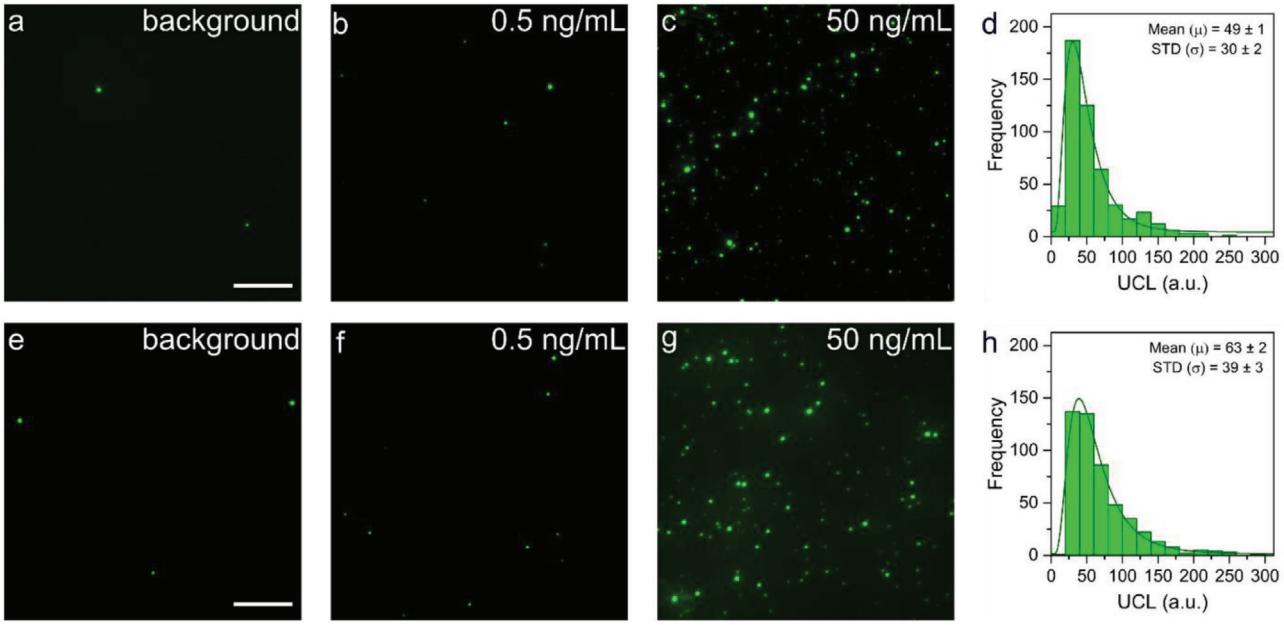

Figure 4. Digital ULISA for the detection of troponin using mAb-PAA-UCNP labels (56 nm in diameter). a–c) Wide-field upconversion microscopy images corresponding to serial dilutions of cTnI in BSA/BGG/IgG buffer. d) Brightness distribution histogram of 500 diffraction-limited spots recorded at 50 ng mL^{-1} of cTnI. e–g) Wide-field upconversion microscopy images corresponding to serial cTnI dilutions in plasma. d) Brightness distribution histogram of 500 diffraction-limited spots recorded at 50 ng mL^{-1} of cTnI in plasma. Scale bar: 10 μm.

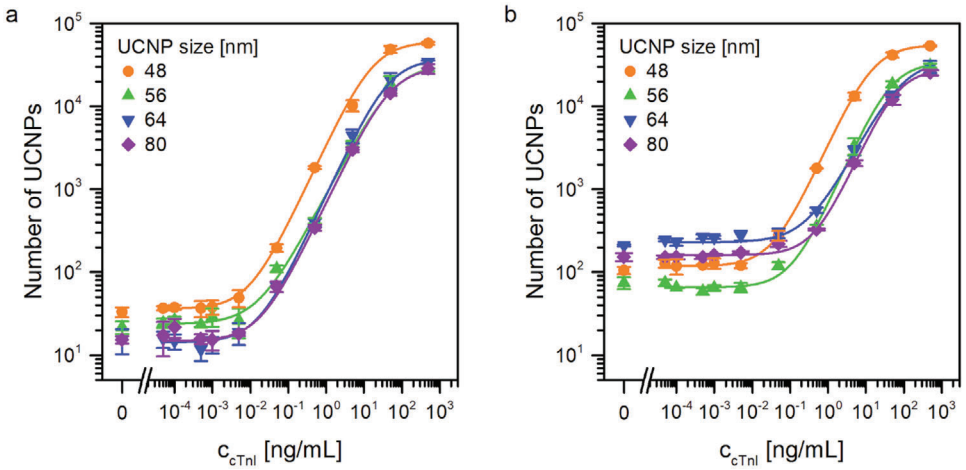

Figure 5. Digital ULISA for the detection of troponin using different sizes of mAb 625cc-PAA-UCNP labels in a) BSA/BGG/IgG buffer and b) 20% plasma. The error bars show the standard deviation of replicate measurements in three wells (mean ± SD, $n = 3$).

the label preparation was more uniform than in our previous PSA assay. Also, the differences in the particular antibody–antigen interactions may explain why the digital assay confers a higher sensitivity only for some analytes. In the analog mode, the PSA assay was ten times more sensitive than the troponin assay. In the digital mode, the PSA assay was even 200 times more sensitive although the number of nonspecifically bound SA-PEG-UCNP labels was ten times higher than the number of mAb-PAA-UCNP labels. Therefore, it seems to be the first requirement that the affinity of the antibody for the analyte is already very high before the sensitivity can be further improved by the digital readout. Compared to commercial cTnI assays and literature reports, however, the ULISA results in a similar or even better assay performance (**Table 2**).

4. Conclusions

For the detection of troponin (cTnI), the advantages conferred by optimizing the assay configuration and the size, brightness, and surface chemistry of UCNP labels were more important than changing from an analog to a digital detection mode. In both cases, an LOD of 10 pg mL^{-1} in human plasma was obtained using mAb-PAA-UCNPs (48 nm in diameter). In contrast to conventional analog measurements, the digital readout allowed

Table 2. Assay platforms for the detection of cTnI.

	Detection label	LOD [pg mL^{-1}]	linear range [ng mL^{-1}]	Company/reference
Commercial assays	Alkaline phosphatase	20	0.00–50.0	Abbott i-STAT[39]
	Alkaline phosphatase	10	0.01–100	Beckman Access 2[40]
	Alkaline phosphatase	10		Beckman Coulter DxI[41]
	Alkaline phosphatase	2.5	0.0023–27000	Beckman Coulter Access hs-cTnI[42]
	Horseradish peroxidase	12		Ortho-Clinical Diagnostics Vitros[43]
	Horseradish peroxidase	100	0.125–8.0	Invitrogen: Human Troponin I (TNNI3) ELISA[44]
Literature reports	5′-6-FAM-modified aptamer	70	0.1–6.0	[45]
	SERS using graphene oxide/gold NP	5	0.01–1000	[46]
	Cyclovoltammetry using whiskered nanofibers	40	0.5–100	[47]
	48-nm UCNP (analog/digital readout)	10	0.04–38 (analog readout)	This work

for distinguishing between the number of nonspecific binding events (observable as the number of diffraction-limited spots) and the degree of label aggregation (observable as an increase in the brightness of individual diffraction-limited spots). In particular, measurements in human plasma were strongly affected by the size of the UCNP labels. While the number of nonspecific binding events strongly increased with the label size, smaller labels led to slightly more aggregated UCNPs. The digital readout also showed that a low background signal is important to achieve a high sensitivity, but ultimately, the digital assay is limited by the counting noise. When comparing different analytes (troponin and PSA) measured under similar experimental conditions, the particular antibody–analyte interaction had a stronger effect on the assay sensitivity than the degree of nonspecific binding.

Supporting Information

Supporting Information is available from the Wiley Online Library or from the author.

Acknowledgements

J.C.B. and K.R. contributed equally to this work. This study was supported by the German Research Foundation (DFG GO 1968/6-2 and Heisenberg Program GO 1968/7-1). Z.F. and P.S. acknowledge financial support from the Ministry of Education, Youth and Sports of the Czech Republic (MEYS CR) under the projects CEITEC 2020 (LQ1601) and INTER-ACTION (LTAB19011). Z.F., A.H., and P.S. acknowledge grant 21-03156S from the Czech Science Foundation. A.H. acknowledges institutional support RVO 68081715 from the Institute of Analytical Chemistry of the Czech Academy of Sciences. K.R. and T.S. acknowledge the funding from Business Finland. CIISB research infrastructure project LM2018127 funded by MEYS CR is acknowledged for the financial support of the measurements at the CF Cryo-electron Microscopy and Tomography, and CF Nanobiotechnology. The authors thank Vít Vykoukal for taking the TEM images and Jaana Rosenberg (Department of Biotechnology, University of Turku) for providing biotin-isothiocyanate.

Open access funding enabled and organized by Projekt DEAL.

Conflict of Interest

The authors declare no conflict of interest.

Data Availability Statement

The data that support the findings of this study are available from the corresponding author upon reasonable request.

Keywords

anti-Stokes emission, cardiac arrest, lanthanide-doped nanomaterials, single molecule immunoassay, troponin

Received: March 16, 2021
Revised: June 22, 2021
Published online:

[1] WHO, www.who.int/data/gho/data/themes/mortality-and-global-health-estimates (accessed: July 2021).
[2] K. Thygesen, J. S. Alpert, A. S. Jaffe, M. L. Simoons, B. R. Chaitman, H. D. White, E. S. C. A. A. H. A. W. H. F. T. F. f. t. U. D. o. M. I. Joint, H. A. Katus, B. Lindahl, D. A. Morrow, P. M. Clemmensen, P. Johanson, H. Hod, R. Underwood, J. J. Bax, R. O. Bonow, F. Pinto, R. J. Gibbons, K. A. Fox, D. Atar, L. K. Newby, M. Galvani, C. W. Hamm, B. F. Uretsky, P. G. Steg, W. Wijns, J. P. Bassand, P. Menasche, J. Ravkilde, E. M. Ohman, E. M. Antman, L. C. Wallentin, P. W. Armstrong, M. L. Simoons, J. L. Januzzi, M. S. Nieminen, M. Gheorghiade, G. Filippatos, R. V. Luepker, S. P. Fortmann, W. D. Rosamond, D. Levy, D. Wood, S. C. Smith, D. Hu, J. L. Lopez-Sendon, R. M. Robertson, D. Weaver, M. Tendera, A. A. Bove, A. N. Parkhomenko, E. J. Vasilieva, S. Mendis, *Circulation* **2012**, *126*, 2020.
[3] S. Takeda, A. Yamashita, K. Maeda, Y. Maeda, *Nature* **2003**, *424*, 35.
[4] I. A. Katrukha, *Biochemistry (Moscow)* **2013**, *78*, 1447.
[5] A. S. Jaffe, J. Ravkilde, R. Roberts, U. Naslund, F. S. Apple, M. Galvani, H. Katus, *Circulation* **2000**, *102*, 1216.
[6] K. Thygesen, J. Mair, H. Katus, M. Plebani, P. Venge, P. Collinson, B. Lindahl, E. Giannitsis, Y. Hasin, M. Galvani, M. Tubaro, J. S. Alpert, L. M. Biasucci, W. Koenig, C. Mueller, K. Huber, C. Hamm, A. S. Jaffe, *Eur. Heart J.* **2010**, *31*, 2197.
[7] D. Westermann, J. T. Neumann, N. A. Sorensen, S. Blankenberg, *Nat. Rev. Cardiol.* **2017**, *14*, 472.
[8] F. S. Apple, Y. Sandoval, A. S. Jaffe, J. Ordonez-Llanos, *Clin. Chem.* **2017**, *63*, 73.
[9] IFCC, https://www.ifcc.org/media/478592/high-sensitivity-cardiac-troponin-i-and-t-assay-analytical-characteristics-designated-by-manufacturer-v072020.pdf (accessed: July 2021).

[10] E. Antman, J. P. Bassand, W. Klein, M. Ohman, J. L. Sendon, L. Rydén, M. L. Simoons, M. Tendera, *J. Am. Coll. Cardiol.* **2000**, *36*, 959.
[11] F. S. Apple, C. A. Parvin, K. F. Buechler, R. H. Christenson, A. H. Wu, A. S. Jaffe, *Clin. Chem.* **2005**, *51*, 2198.
[12] A. G. Katrukha, A. V. Bereznikova, V. L. Filatov, T. V. Esakova, O. V. Kolosova, K. Pettersson, T. Lovgren, T. V. Bulargina, I. R. Trifonov, N. A. Gratsiansky, K. Pulkki, L. M. Voipio-Pulkki, N. B. Gusev, *Clin. Chem.* **1998**, *44*, 2433.
[13] M. Panteghini, W. Gerhardt, F. S. Apple, F. Dati, J. Ravkilde, A. H. Wu, *Clin. Chem. Lab. Med.* **2001**, *39*, 175.
[14] M. Panteghini, *Clin. Chim. Acta* **2009**, *402*, 88.
[15] D. S. Herman, P. A. Kavsak, D. N. Greene, *Am. J. Clin. Pathol.* **2017**, *148*, 281.
[16] F. S. Apple, P. O. Collinson, I. T. F. o. C. A. o. C. Biomarkers, *Clin. Chem.* **2012**, *58*, 54.
[17] C. Chenevier-Gobeaux, E. Bonnefoy-Cudraz, S. Charpentier, M. Dehoux, G. Lefevre, C. Meune, P. Ray, S. F. C. S. T. w. Sfbc, *Arch. Cardiovasc. Dis.* **2015**, *108*, 132.
[18] Z. Farka, T. Jurik, D. Kovar, L. Trnkova, P. Skladal, *Chem. Rev.* **2017**, *117*, 9973.
[19] Z. Farka, M. J. Mickert, A. Hlavacek, P. Skladal, H. H. Gorris, *Anal. Chem.* **2017**, *89*, 11825.
[20] A. Hlavacek, Z. Farka, M. Hubner, V. Hornakova, D. Nemecek, R. Niessner, P. Skladal, D. Knopp, H. H. Gorris, *Anal. Chem.* **2016**, *88*, 6011.
[21] V. Polachova, M. Pastucha, Z. Mikusova, M. J. Mickert, A. Hlavacek, H. H. Gorris, P. Skladal, Z. Farka, *Nanoscale* **2019**, *11*, 8343.
[22] R. Peltomaa, Z. Farka, M. J. Mickert, J. C. Brandmeier, M. Pastucha, A. Hlavacek, M. Martinez-Orts, A. Canales, P. Skladal, E. Benito-Pena, M. C. Moreno-Bondi, H. H. Gorris, *Biosens. Bioelectron.* **2020**, *170*, 112683.
[23] U. Kostiv, V. Lobaz, J. Kucka, P. Svec, O. Sedlacek, M. Hruby, O. Janouskova, P. Francova, V. Kolarova, L. Sefc, D. Horak, *Nanoscale* **2017**, *9*, 16680.
[24] Z. Farka, M. J. Mickert, Z. Mikusova, A. Hlavacek, P. Bouchalova, W. Xu, P. Bouchal, P. Skladal, H. H. Gorris, *Nanoscale* **2020**, *12*, 8303.
[25] L. Xiong, T. Yang, Y. Yang, C. Xu, F. Li, *Biomaterials* **2010**, *31*, 7078.
[26] M. J. Mickert, Z. Farka, U. Kostiv, A. Hlavacek, D. Horak, P. Skladal, H. H. Gorris, *Anal. Chem.* **2019**, *91*, 9435.
[27] Z. Farka, M. J. Mickert, M. Pastucha, Z. Mikusova, P. Skladal, H. H. Gorris, *Angew. Chem., Int. Ed. Engl.* **2020**, *59*, 10746.
[28] S. Lahtinen, A. Lyytikainen, N. Sirkka, H. Pakkila, T. Soukka, *Mikrochim. Acta* **2018**, *185*, 220.
[29] N. Sirkka, A. Lyytikainen, T. Savukoski, T. Soukka, *Anal. Chim. Acta* **2016**, *925*, 82.
[30] S. Eriksson, M. Junikka, P. Laitinen, K. Majamaa-Voltti, H. Alfthan, K. Pettersson, *Clin. Chem.* **2003**, *49*, 1095.
[31] J. Ylikotila, J. L. Hellstrom, S. Eriksson, M. Vehniainen, L. Valimaa, H. Takalo, A. Bereznikova, K. Pettersson, *Clin. Biochem.* **2006**, *39*, 843.
[32] M. Pastucha, E. Odstrcilikova, A. Hlavacek, J. C. Brandmeier, V. Vykoukal, J. Weisova, H. H. Gorris, P. Skladal, Z. Farka, *IEEE J. Sel. Top. Quantum Electron.* **2021**, *27*, 1.
[33] S. Lahtinen, M. Baldtzer Liisberg, K. Raikko, S. Krause, T. Soukka, T. Vosch, *ACS Appl. Nano Mater.* **2021**, *4*, 432.
[34] L. Välimaa, K. Pettersson, M. Vehniäinen, M. Karp, T. Lövgren, *Bioconjug. Chem.* **2003**, *14*, 103.
[35] A. Sedlmeier, A. Hlavacek, L. Birner, M. J. Mickert, V. Muhr, T. Hirsch, P. L. Corstjens, H. J. Tanke, T. Soukka, H. H. Gorris, *Anal. Chem.* **2016**, *88*, 1835.
[36] T. Savukoski, J. Jacobino, P. Laitinen, B. Lindahl, P. Venge, N. Ristiniemi, S. Wittfooth, K. Pettersson, *Clin. Chem. Lab. Med.* **2014**, *52*, 1041.
[37] T. Savukoski, A. Twarda, S. Hellberg, N. Ristiniemi, S. Wittfooth, J. Sinisalo, K. Pettersson, *Clin. Chem.* **2013**, *59*, 512.
[38] A. G. Katrukha, in *Cardiac Markers* (Ed.: A. H. B. Wu), 2nd Ed., Humana Press, Totowa, NJ **2002**, pp. 173.
[39] G. Bozkaya, A. R. Sisman, *Ann. Transl. Med.* **2020**, *8*, 1237.
[40] F. S. Apple, Y. Sandoval, A. S. Jaffe, J. Ordonez-Llanos, *Clin. Chem.* **2017**, *63*, 73,.
[41] F. S. Apple, M. M. Murakami, *Clin. Chem.* **2007**, *53*, 1558.
[42] S. Kim, S. J. Yoo, J. Kim, *Clin. Biochem.* **2020**, *79*, 48.
[43] F. S. Apple, R. Ler, A. Y. Chung, M. J. Berger, M. M. Murakami, *Clin. Chem.* **2006**, *52*, 322.
[44] https://www.thermofisher.com/elisa/product/Cardiac-Troponin-I-TNNI3-Human-ELISA-Kit/EHTNNI3 (accessed: July 2021).
[45] D. Liu, X. Lu, Y. Yang, Y. Zhai, J. Zhang, L. Li, *Anal. Bioanal. Chem.* **2018**, *410*, 4285.
[46] X. L. Fu, Y. Q. Wang, Y. M. Liu, H. T. Liu, L. W. Fu, J. H. Wen, J. W. Li, P. H. Wei, L. X. Chen, *Analyst* **2019**, *144*, 1582.
[47] B. Rezaei, A. M. Shoushtari, M. Rabiee, L. Uzun, W. C. Mak, A. P. F. Turner, *Talanta* **2018**, *182*, 178.